

# Reduced ARAIM monitoring subset method based on satellites in different orbital planes

Yishan Ge<sup>1</sup> · Zhipeng Wang<sup>1</sup> · Yanbo Zhu<sup>1</sup>

Received: 13 February 2017 / Accepted: 11 August 2017 / Published online: 29 August 2017  
© Springer-Verlag GmbH Germany 2017

**Abstract** With the development of the Global Navigation Satellite System, the increased number of satellites has resulted in more fault hypothesis situations and subset solutions. This situation represents a new challenge for advanced receiver autonomous integrity monitoring (ARAIM) in terms of the computational load. To efficiently detect faults and reduce the computational load, a method based on the association between satellite features in the same orbital plane is proposed. This approach first tests subsets that exclude entire constellations to narrow the search range for faults. Next, we evaluate multiple-fault cases directly by utilizing the subsets that exclude entire orbit satellites. Compared with the baseline Multiple Hypothesis Solution Separation (MHSS) method, our method can clearly reduce the number of subsets and the computational time under a typical multi-constellation situation while satisfying the localizer precision vertical 200 performance requirement, i.e., the guidance supports approach operations down to 200-foot altitudes. Furthermore, the experimental results illustrate that the number of subsets is reduced at most by two orders of magnitude, from 1330 to 87, and the computational time is decreased by 66.6%. The effective monitoring threshold and the fault-free  $10^{-7}$  error bound on the accuracy of our method are much closer to those of the baseline MHSS method, and the usability coverage of both methods reaches 100%. This study verifies that the monitoring subsets and the

calculation time for ARAIM are dramatically reduced by the new method.

**Keywords** ARAIM · Fault detection · Monitoring subset · Orbit satellite

## Introduction

Integrity monitoring is a key link in safety of life applications used to ensure Global Navigation Satellite System (GNSS) spatial signal quality. Advanced receiver autonomous integrity monitoring (ARAIM), as a typical airborne integrity monitoring technology (GEAS 2008, 2010), can effectively monitor navigation performance through redundant satellite measurements, rapidly detect and exclude satellite faults, and alarm the user in time (Wang and Ober 2009). With the development of the Global Positioning System (GPS), GLONASS (the Russian GNSS), BeiDou Navigation Satellite System (BDS) and Galileo, the number of visible satellites is bound to increase, thereby improving the positioning accuracy and service reliability. Moreover, higher numbers of constellations and satellites also correspond to a greater number of GNSS potential failure modes. The Multiple Hypothesis Solution Separation (MHSS) algorithm (Blanch et al. 2012; Working Group C 2012) is the basis of the ARAIM user algorithm. This baseline MHSS method, which is used widely, detects the failure modes by comparing the all-in-view position solution and the subset solutions with the assumed-to-be faulty satellite removed. For multiple constellations, many more subsets must be evaluated by the ARAIM receiver, thus greatly increasing the computational load. Therefore, it is necessary to reduce the monitoring subsets for future applications.

✉ Zhipeng Wang  
wangzhipeng@buaa.edu.cn

<sup>1</sup> National Key Laboratory of CNS/ATM, School of Electronic and Information Engineering, Beihang University, Beijing 100191, China

To date, the only method developed to address this problem is the Constellation Out (ConOut) method presented by Walter et al. (2014). In this approach, subsets that remove whole constellations are ingeniously used to evaluate multiple-fault cases, which effectively reduces the total number of subsets. However, removal of whole constellations will lead to a rapidly weakening geometry, which may not be conducive to system operation, particularly if one of the constellations is weak.

The trajectory of a satellite in space is called an orbit, and the parameters describing the orbital position and state of the satellite are referred to as the orbital parameters. When we use a GNSS for navigation and surveying purposes, the satellite orbit error will directly affect the accuracy of the user receiver position solution. In practice, a satellite will be impacted by some perturbation forces. These forces cause the satellite motion to deviate from the ideal trajectory predicted by Kepler's law for a "two-body problem." Under the influence of such perturbation forces, only satellites in the same orbital plane have similar orbital parameter changes. Therefore, when predicting the satellite ephemeris at the observation epoch based on the broadcast ephemeris, the orbital parameters of the orbiting satellites are highly correlated, including bias (Liu 2008, p. 82).

Combining the ARAIM baseline MHSS method and the ConOut method, we propose an Orbit Selection (OrbSel) method that can effectively reduce the subsets according to the kinematic properties satellites in the same orbital plane. To evaluate and eliminate potential multiple faults existing in orbital satellites, we divide subsets according to different satellite orbit planes. This approach is also beneficial for rapid fault detection. The OrbSel method preserves geometry better than does directly removing the entire constellation. Finally, we compare the number of subsets and the computational expense of the three methods. Simulation results regarding the availability of ARAIM are also provided.

## ARAIM framework

ARAIM allows a ground system to provide updates regarding the nominal performance and fault rates of the multiplicity of contributing constellations. This integrity data is contained in the Integrity Support Message (ISM), which is developed on the ground and provided to the airborne fleet. The key input of the ARAIM user algorithm is shown in Table 1.

ARAIM allows for the possibility that some of the ranging measurements that are made to the satellites may be incorrectly described by the parameters  $\sigma_{URA,i}$ ,  $\sigma_{URE,i}$  and  $b_{nom,i}$ . If a satellite is in a state in which these are not

accurate descriptions of the expected pseudorange errors, the satellite is considered faulty. The receiver determines which fault modes need to be monitored from  $P_{sat,i}$  and  $P_{const,i}$  of the ISM. Each fault mode corresponds to a subset that removes some of the satellites presumed to be faulty.

ARAIM ensures integrity by comparing the position solution estimated with all satellites in view to estimates from subsets. If each of the solution separations between the all-in-view and the fault tolerant position solution is within a predefined threshold, then the receiver computes the following:

- Protection levels (PLs)
- Effective monitor threshold (EMT)
- Standard deviation of the accuracy ( $\sigma_{acc}$ )

The sum of the threshold and the subset covariance error bound is sufficient, and the all—in-view position error will be bounded by the PLs. The EMT ensures that the internal threshold is sufficiently tight.  $\sigma_{acc}$  presents 99.99999% fault-free accuracy. All calculation formulas can be found in Blanch et al. (2012).

If the solution separations exceed the threshold, the protection levels are set to infinity. Then, exclusion is attempted, and the above steps are continuously performed using the remaining satellites. Exclusion is beyond the scope of our discussion.

## Ephemeris errors of satellites in the same orbital plane

Navigation threats are considered all possible events that can cause the computed navigation solution to deviate from the true position. The set of possible events can be separated into the following three categories: Narrow, Wide, and Ultra-Wide. Narrow faults are ones that affect a single satellite only. Wide faults are ones that can affect more than one satellite within a constellation at a given time. These are also called constellation faults. Ultra-Wide faults are those that can affect multiple satellites across more than one constellation, e.g., the Earth Orientation Prediction Parameters (EOPPs) error (Langel et al. 2013). However, there are many processes in place that greatly reduce the likelihood of ultra-wide faults affecting all constellations in a similar manner simultaneously (van Dyke et al. 2004). Hence, we do not further consider ultra-wide faults.

An ephemeris error, as the main source of error for satellite navigation positioning, may lead to narrow faults and wide faults. The satellite ephemeris, translated from satellite navigation messages, is called the satellite broadcast ephemeris. It is "extrapolated" from the broadcast data. The ephemeris error is mainly due to the complexity

**Table 1** List of input

| Name             | Description   | Source   |
|------------------|---|----------|
| $PR_i$           | Pseudorange for satellite $i$ after dual frequency correction tropospheric correction and smoothing are performed | Receiver |
| $\sigma_{URA,i}$ | Standard deviation of the clock and ephemeris error of satellite $i$ used for integrity                           | ISM      |
| $\sigma_{URE,i}$ | Standard deviation of the clock and ephemeris error of satellite $i$ used for continuity                          | ISM      |
| $b_{nom,i}$      | Maximum nominal bias of satellite $i$ used for integrity  | ISM      |
| $P_{sat,i}$      | Prior probability of satellite $i$ fault  | ISM      |
| $P_{const,j}$    | Prior probability of constellation $j$ fault  | ISM      |

and instability of satellite orbit perturbations, which can lead to wide faults associated with the satellite orbital planes (Liu 2008, p. 82). In the geocentric reference system, the motion equation of a satellite traveling around the earth can be written as

$$\ddot{r} = F_0 + F_\epsilon \tag{1}$$

where  $F_0$  is the earth-center gravitational and  $F_\epsilon$  represents perturbation forces including earth’s non-spherical gravity, third-body gravity, and solar radiation pressure (Kaula 1966, p. 124).

**Heterogeneous constellation**

A heterogeneous constellation consists of satellites of different orbital types. The Chinese BDS is a typical heterogeneous constellation. After completion, the BDS will comprise 35 satellites, of which five Geostationary Orbit (GEO) satellites will be in one orbit, three Inclined Geosynchronous Satellite Orbit (IGSO) satellites will be distributed in three different orbits, and 27 Medium Earth Orbit (MEO) satellites will be distributed in three orbits, with nine satellites in each orbit. The perturbed motions of the three kinds of orbiting satellites have different characteristics. Regarding GEO satellites, the orbit inclination is close to 0° and the altitude is approximately 35,800 km. They are maneuvered more frequently, with an ephemeris fault probability slightly higher than that of other satellites (Cui et al. 2012). IGSO satellites have a regressive orbit of a sidereal day that is affected by the tesseral harmonic terms of earth’s gravity, which can produce long-term drift (Fan et al. 2016). Regarding MEO satellites, please refer to the isomorphic constellation section below.

**Isomorphic constellation**

An isomorphic constellation consists of satellites of the same orbital type satellites. GPS, Galileo, and GLONASS are all isomorphic constellations consisting of MEO satellites distributed over 6, 3, and 3 orbit planes,

respectively. The influence of the perturbation forces on the orbit stability of MEO satellites is mainly as follows (Rippl 2013):

- No long-term effect on the semi-major axis  $a$ , eccentricity  $e$  and inclination  $i$
- Long-term perturbation of the Right Ascension of Ascending Node (RAAN)  $\Omega$ , argument of perigee  $\omega$  and mean anomaly  $M$

Therefore, damage to the stability of a constellation is mainly manifested in  $(\Omega, \omega, M)$ , and the structural stability of the circular orbit satellite constellation can be described by the drift of  $(\Omega, \omega, M)$ .

In the MEO constellation, the deviation of the actual state  $(\Omega_j, u_j)$  and the nominal state  $(\Omega_{j,norm}, u_{j,norm})$  for the  $j$ th satellite is

$$\Delta x_j = \begin{bmatrix} \Omega_j - \Omega_{j,norm} \\ u_j - u_{j,norm} \end{bmatrix} = \begin{bmatrix} \Delta \Omega_j \\ \Delta u_j \end{bmatrix} \tag{2}$$

where  $u = \omega + M$  is the phase angle of satellite  $j$  on the orbital plane. The common drift of the RAAN and phase angles of the constellation satellite is defined as

$$\begin{cases} \Delta \Omega = \sum_{j=1}^N \frac{\Delta \Omega_j}{N} \\ \Delta u = \sum_{j=1}^N \frac{\Delta u_j}{N} \end{cases} \tag{3}$$

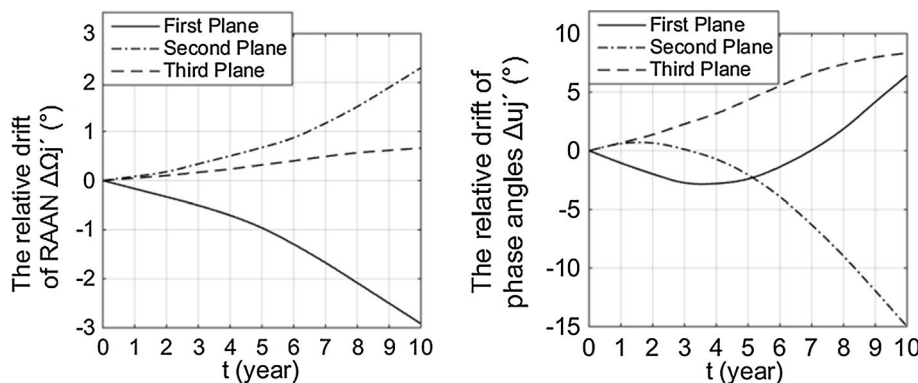
where  $N$  is the total number of satellites in the constellation. The deviation subtracts the common drift amount to obtain the relative drift  $\Delta x'_j$  of satellite  $j$

$$\Delta x'_j = \begin{bmatrix} \Delta \Omega'_j \\ \Delta u'_j \end{bmatrix} = \begin{bmatrix} \Delta \Omega_j - \Delta \Omega \\ \Delta u_j - \Delta u \end{bmatrix} \tag{4}$$

The relative drift of the satellite can be used to describe the change of the spatial configuration state of the MEO constellation (Qian et al. 2014).

Figure 1 shows the relative drifts of  $\Omega$  and  $u$  for a 24/3/1 Walker constellation with the perturbation effect (Starr et al. 2004). 24 is the total number of satellites, 3 is the number of orbital planes, and 1 is the value of the phase

**Fig. 1** Relative drifts of the RAAN and phase angles for a 24/3/1 Walker constellation with the perturbation effect over 10 years



factor (Walker 1984). The inclination is 55°, the orbital height is 21,500 km, and the initial values RAAN of the three orbital planes are 0°, 120°, and 240°.

Under the action of the main perturbation forces, the relative drift of the RAAN of the same orbital plane is basically the same, and the relative change in the RAAN of different orbiting satellites corresponds to a linear increase with time. The relative drift of the same orbital satellite phase is basically the same; the phase angle of different orbiting satellites is different from the drift amount, with the maximum drift being 15°.

Even if the Constellation Service Providers (CSP) control the perturbation compensation for their own constellations, the long-term effect of perturbation forces is still the main source of ephemeris errors, leading to wide faults within constellations (Shah et al. 1998). The fault hypothesis that all orbital plane satellites are affected is feasible.

**ARAIM fault modes determination**

ARAIM, a technique used for rapid navigation satellite fault monitoring to ensure flight safety, solves two main problems: (1) determining whether a failure occurs among satellites/constellations and (2) determining in which satellites/constellations the fault exists. The former problem is often referred to as fault detection (FD), and the latter problem is fault exclusion (FE). In the ARAIM baseline MHSS method, the approach of ARAIM FD involves the following tasks: fault assumption, subset position solution calculation and solution separation threshold tests (Blanch et al. 2012). The fault assumption, which includes determination of the fault that must be monitored (corresponding to the number of subsets), is a key part of the ARAIM FD and can impact the performance of the entire algorithm (GEAS 2008). Many hypotheses provide full consideration but require much computation and time consumption. In the future, the ARAIM algorithm must be able to determine how to

achieve maximum performance benefits based on the fault modes assumptions and time consumption.

**Failure modes and monitoring subsets**

The airborne ARAIM algorithm can only protect the user against a limited number of worst-case simultaneous satellite faults. If the prior probability of a fault is greater than or equal to  $4 \times 10^{-8}$ , it cannot be ignored and must be monitored by the receiver (Blanch et al. 2012).

The prior probability of a fault mode is calculated as follow, assuming that the probabilities of satellite faults are the same,

$$P_{ap,n_s} = C_N^{n_s} (P_{sat,i})^{n_s} (1 - P_{sat,i})^{N-n_s} \tag{5}$$

$$P_{ap,n_c} = C_M^{n_c} (P_{const,j})^{n_c} (1 - P_{const,j})^{M-n_c} \tag{6}$$

where  $n_s/n_c$  represents the number of satellites/constellations that are simultaneously faulty, and it is assumed that the user is tracking  $N$  satellites belonging to  $M$  constellations.  $C_b^a$  is a combination formula that indicates the total number of combinations of  $a$  elements taken from  $b$  different elements; the calculating method is  $\frac{b!}{a!(b-a)!}$ .

Then, the maximum number of monitored simultaneous faults can be determined.  $N_{sat}$  represents the number of satellites, and  $N_{const}$  denotes the number of constellations,

$$N_{sat} = \max\{n_s | 1 - (P_{ap,0} + P_{ap,1} + \dots + P_{ap,n_s}) \leq 4 \times 10^{-8}\} \tag{7}$$

$$N_{const} = \max\{n_c | 1 - (P_{ap,0} + P_{ap,1} + \dots + P_{ap,n_c}) \leq 4 \times 10^{-8}\} \tag{8}$$

where  $P_{sat,i}$  and  $P_{const,j}$  are input parameters acquired from the Integrity Support Message (ISM) obtained by the receiver;  $4 \times 10^{-8}$  is a constant used in ARAIM as a threshold for the integrity risk resulting from unmonitored faults (Kropp et al. 2014). To illustrate, assume that the user is tracking three constellations and that  $P_{const}$  is  $10^{-4}$ . Then, we have

$$[1 - (P_{ap,0} + P_{ap,1})] = 2.99 \times 10^{-8} \leq 4 \times 10^{-8} \tag{9}$$

Therefore, the maximum number of simultaneous constellations  $N_{const}$  is one. The calculation of  $N_{sat}$  is the same.

According to the derived  $N_{sat}$  and  $N_{const}$ , we can make assumptions regarding the failure modes. Each fault hypothesis corresponds to a monitoring subset. Thus, if the  $k$ th satellite is assumed to be faulty, then a corresponding subset that excludes satellite  $k$  will be formed (Blanch et al. 2012).

Figure 2 shows the baseline MHSS method fault tree. In this approach, all possible fault conditions must be considered. All single fault assumptions (including satellite faults and constellation faults) and multi-faults assumptions will be made in order by means of ergodic, until the upper simultaneous faults limit  $N_{sat}/N_{const}$ . Next, the fault monitoring subsets will be established corresponding to the hypothesis with satellites or constellations excluded. In most cases, the probability of occurrence of three and more simultaneous failure events is always less than  $10^{-7}$  and can be neglected (Walter et al. 2014). Suppose that the number of constellations tracked by the user receiver is 4, the number of visible satellites is 48 and the maximum number of monitored simultaneous faults is 2 ( $N_{sat}/N_{const} = 2$ ); then, a total of  $(C_{48}^1 + C_4^1) + (C_{48}^2 + C_{48}^1 C_3^1 + C_4^2) = 1330$  subsets must be created by the baseline MHSS method. Although subset-filtering measures are contained in the baseline MHSS method, the number of subsets is still greater than 1000.

**Subset position solution and threshold test of solution separation**

In this part, the subset solutions  $\hat{x}^{(k)}$ , the corresponding standard deviations, bias and the standard deviations of solution separation  $\sigma_{ss}^{(k)}$  for more than 1000 subsets will be

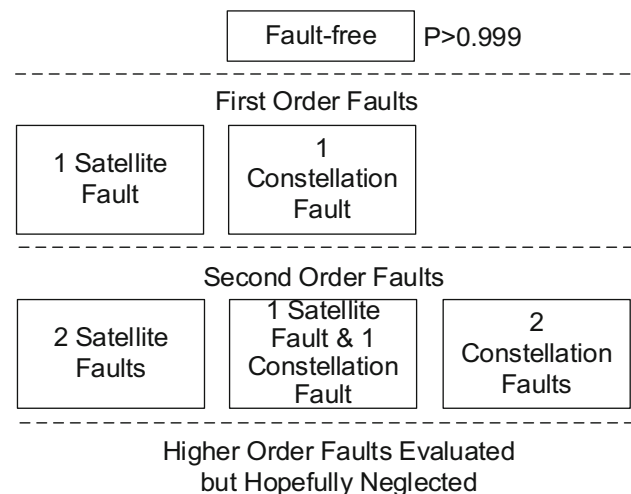


Fig. 2 Baseline MHSS method fault tree

calculated, i.e., more than four operations on each subset will be performed. With the increase in the number of subsets, more operations and computational time will be needed. Subsequently, the subset position solution and all-in-view solution  $\hat{x}^{(0)}$  are compared to determine whether exclusion must be attempted. This step is the threshold test, also known as a consistency check, in which items with large differences with respect to  $\hat{x}^{(0)}$  are checked.

$$\tau_k = \frac{|\hat{x}^{(k)} - \hat{x}^{(0)}|}{T_k} \leq 1 \tag{10}$$

$$T_{k,q} = K_{fa,q} \sigma_{ss,q}^{(k)2} \tag{11}$$

$$K_{fa} = Q^{-1} \left( \frac{P_{FA}}{2N_{fault\_modes}} \right) \tag{12}$$

where  $N_{fault\_modes}$  is the number of subsets,  $P_{FA}$  is the continuity budget allocated to the  $q$  direction component, and  $Q^{-1}(p)$  is the  $(1 - p)$  quantile of the standard Gaussian distribution. If the test statistic  $\tau_k$  in (11) is greater than one, then the test fails and exclusion must be attempted (Working Group C 2016).

Currently, there exist four normal operation navigation constellations. If there appear new navigation constellations in the future, then the number of satellites will increase dramatically. In this case, the system will possess high positioning accuracy but significantly increase the ARAIM computational time, which is not beneficial for forecasting and obtaining real-time solutions.

**ConOut method to select subsets**

Walter et al. (2014) described a method that directly removes an entire constellation as a subset to evaluate other possible failure modes within the constellation. This approach can greatly reduce the number of subsets. The number of subsets obtained by this method is determined according to the concrete values of  $P_{sat,i}$  and  $P_{const,j}$ . In the following discussion,  $P_{const,j}$  is restricted such that it ranges between  $10^{-3}$  and  $10^{-5}$ , while  $P_{sat,i}$ , between  $10^{-4}$  and  $10^{-6}$ .

When the receiver uses double constellations, the situation in which both constellations are faulted simultaneously cannot be avoided. In addition, it is not possible to use the two-constellation-out cases to evaluate the two-satellite-fault cases. These cases must be evaluated directly or as part of a one-constellation-out and one-satellite-out subset. However, this method can cause some of the most valuable satellites to be removed, which will result in poor geometry and lead to lower availability. When  $P_{const,j} = 10^{-3}$ , the two constellations cannot safely function; when  $P_{const,j}$  is small and  $P_{sat,i} = 10^{-4}$ , all first-order modes should be evaluated individually. When  $P_{sat,i}$  is even



smaller, it is possible to evaluate only the two one-constellation-out subsets.

For the three-constellation situation, it is possible to evaluate the two-constellation-out subsets, but only one constellation may have a poor geometry. However, only one constellation may not always have good geometry, particularly if one of the constellations is weak. For  $P_{\text{const},j} = 10^{-3}$ , we need to evaluate only the three one-constellation-out and three two-constellations-out subsets. For  $P_{\text{const},j} = 10^{-4}$ , three two-constellations-out and  $2N$  one-constellation-out and one-satellite-out subsets are recommended. If  $P_{\text{sat},i}$  and  $P_{\text{const},j}$  are sufficiently small, evaluating only three one-constellation-out subsets becomes possible.

When the receiver uses four constellations, the geometric relationship is strong. The four one-constellation-out and six two-constellation-out subsets are recommended in most of the cases. The main challenge of the ConOut method is to preserve the geometric integrity when an entire constellation is removed. Recall that FE is beyond the scope of this work; for example, in the two-constellation case, two one-constellation-out subsets can detect the presence of a fault but not exclude it.

### Reducing monitoring subsets based on the selection of orbit satellites

Because co-orbital satellites have related kinematic properties and the number of orbits will increase slowly in the future, the monitoring subsets can be determined by selecting an orbital plane and removing its satellites.

We present the OrbSel method on the basis of 2-order fault tree. Fault assumptions are made in turn for each of the orders. To express the method more clearly, Fig. 3 shows the fault tree, where “Constellation Fault” mode indicates that one or more satellite faults occur within a

given constellation at the same time and “Orbit Fault” mode indicates that one or more satellite faults occur in a given orbit at the same time.

### Subsets for the constellation order

The first order is the constellation order. First, determine the maximum number of simultaneous constellation faults  $N_{\text{const}}$  using (9). Next, the fault modes and the subsets evaluated by constellation order are determined. Note that the prior probability of constellation fault should be calculated by (Walter et al. 2014)

$$P_{\text{const},j} = P_{\text{const},j} + \sum_{i=1}^{N_j} P_{\text{sat},i} \tag{13}$$

Clearly, if  $N_{\text{const}} = 3$ , the receiver should track at least four constellations. In this case, three synchronous constellations faults are assumed; the faults are distributed in no more than three constellations. Thus, we obtain four one-constellation-out, six two-constellation-out, and four three-constellation-out subsets.

In this part, the subset position solution  $\hat{x}^{(k)}$  and the standard deviation of the solution separation  $\sigma_{\text{ss}}^{(k)}$  for the above subsets are computed. In addition,  $\hat{x}^{(k)}$  is compared to the all-in-view solution  $\hat{x}^{(0)}$  for the threshold test. The traditional calculation formulas are (11), (12) and (13). We make an optimal allocation of the continuity risk in (12) based on the number of satellites in each subset rather than the average distribution. The updated formula is

$$P_{\text{FA}}^{(k)} = P_{\text{FA}} \cdot \frac{n_k}{n}, \quad k = 1, 2, \dots \tag{14}$$

where  $n_k$  is the number of visible satellites contained in the subset  $k$ ,  $n$  is the number of visible satellites and  $P_{\text{FA}}$  is the continuity budget allocated to the specific directional component. The subset of constellation order that does not pass the threshold test or has the largest test statistic will be selected, indicating that the satellites corresponding to the fault mode are faulty or very likely to be faulty. To facilitate rapid fault detection and elimination, we determine the fault modes and subsets in orbit order of the constellation(s) that are assumed to be faulty of the selected subset. The fault mode hypothesis corresponding to the other constellation order subsets is unlikely to make more fault assumptions. Therefore, they all can be used in position.

### Subsets for orbit order

Because only BDS consists of MEO, IGSO, and GEO hybrid orbit satellites, the other navigation constellations are composed of MEO satellites, there are slight

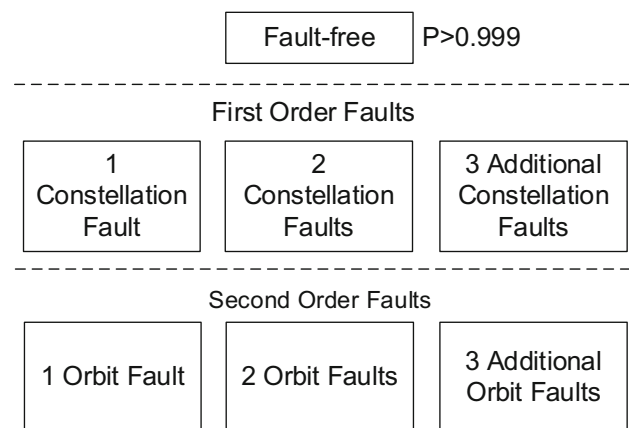


Fig. 3 OrbSel method fault tree

differences in subset selection for areas covered by IGSO and GEO satellites of BDS.

Similar to the constellation order, the maximum number of simultaneous satellites faults  $N_{\text{sat}}$  is initially determined as specified in (8). If  $N_{\text{sat}} = 1$ ,  $N_{\text{orbit}}$ , i.e., the number of orbits of the selected constellation(s) in the previous step, can be determined. Each orbit subset is used to evaluate all single satellite fault modes in the orbit. If  $N_{\text{sat}} = 2$ , there may be at most two satellite faults at the same time; thus, we can obtain  $C_{N_{\text{orbit}}}^2$  two orbit-outs subsets. Regardless of whether the two fault satellites are co-orbiting satellites or different orbiting ones, our subset can evaluate all possible two faults modes between orbits directly. The steps are similar when  $N_{\text{sat}}$  equals to or greater than three, but the probability of this situation is so small that it can be ignored.

Because the orbit subset corresponds to one or more satellite faults in the removed orbit, the prior probability of removing the satellites of an entire orbit can be written as

$$P_{\text{orbit},m} = \sum_{i=1}^{N_m} P_{\text{sat},i} \tag{15}$$

where  $n_m$  represents the satellites in the orbit used by the receiver for positioning. At this point, all subsets of the OrbSel method are created. Next, expressions (7), (8) and (9) are calculated. The continuity risk in (6) can be derived by multiplying (8) by a coefficient as follows:

$$P_{\text{FA}}^{(km)} = P_{\text{FA}}^{(k)} \cdot \frac{n_{km}}{n_k} = P_{\text{FA}} \cdot \frac{n_{km}}{n}, \quad m = 1, 2, \dots \tag{16}$$

where  $n_{km}$  is the number of visible satellites in the excluded orbit  $m$ .

For the areas observed by the IGSO and GEO satellites of BDS, we can simultaneously remove five GEO satellites of the same orbit in one subset to evaluate the faults directly. The three IGSO satellites with different orbits can be removed simultaneously because satellites with such orbits can be considered as a class. Therefore, one three-IGSO-out subset can be effectively utilized, but not several different IGSO subsets. Such subsets can fully verify the validity of the single/multiple-fault assumptions for GEO and IGSO.

Table 2 lists the worldwide statistical results regarding subsets for the baseline MHSS, ConOut and OrbSel methods in different situations. For statistical generality, we set  $P_{\text{sat},i} = 10^{-5}$ ,  $P_{\text{const},j} = 10^{-4}$  (Working Group C 2016).

As shown in Table 2, both the ConOut and OrbSel methods reduce the number of monitoring subsets to some extent. In the case of multiple constellations, the effectiveness of the ConOut method is more obvious. Nevertheless, the performance depends on the follow-up simulation results.

### ARAIM availability prediction

ARAIM fault detection and exclusion mainly depend on the satellite geometry and the input conditions. To ensure the performance requirements of fault detection and exclusion, the prediction of the availability of ARAIM has become an important topic (Zhi et al. 2016).

At a certain space–time point, an available system means it can meet the alarm threshold, integrity and availability requirements. In contrast, a system is unavailable once one or several indicators cannot be met (Wang et al. 2014). Today’s popular ARAIM availability prediction algorithms mainly compare computational protection levels (PLs) with alert limits (ALs) to predict ARAIM availability, with the integrity and availability requirements as known values (Working Group C 2012).

ARAIM operational objectives tend to focus on the Localizer Precision Vertical (LPV) goal, especially LPV-200, which indicates that this guidance should support approach operations down to 200-foot altitudes (Working Group C 2015). The LPV-200 performance standard for ARAIM availability prediction can be summarized as follows:

- $\text{HPL} \leq 40 \text{ m}$
- $\text{VPL} \leq 35 \text{ m}$
- $\sigma_{\text{acc}} \leq 1.87 \text{ m}$
- $\text{EMT} \leq 15 \text{ m}$

where H/VPL denotes the Horizontal/Vertical Protection Level and the limit on the position error is 99.99999%;  $\sigma_{\text{acc}}$  is the standard deviation of the position solution under the  $10^{-7}$  fault-free positional error bound. The effective monitoring threshold (EMT) test prevents faults that are not sufficiently large to be detected from creating vertical position errors greater than 15 m more than 0.00001% of the time (Lee and McLaughlin 2007). ARAIM is considered to be available in the corresponding environment and LPV-200 operation, while the above index criteria calculated by the ARAIM prediction algorithm are satisfied.

In the previous sections, the numbers of subsets of the three methods for determining ARAIM monitoring subsets were compared. The numbers of subsets for both the ConOut and OrbSel methods are two orders of magnitude less than the number of subsets for the baseline MHSS method (10 and 78 vs. 1330). Next, to further validate the availability of ARAIM after using three methods, the availability prediction will be performed.

Table 3 lists the simulation configuration. The nominal 24 satellites GPS constellation, the nominal 24 satellites GLONASS constellation, the global 30 Galileo satellites constellation, and the global 35 BDS satellites constellation will be used separately for various simulation situations.

**Table 2** Comparison of subsets for three methods

| $P_{\text{sat},i} = 10^{-5}$ ,<br>$P_{\text{const},j} = 10^{-4}$ | Baseline method | ConOut method | OrbSel method |
|--|-----------------|---------------|---------------|
| Two constellation  |                 |               |               |
| 16 SVs   | 19              | 2             | 7             |
| 24 SVs   | 26              | 2             | 9             |
| Three constellation  |                 |               |               |
| 24 SVs   | 379             | 51            | 49            |
| 36 SVs   | 781             | 75            | 75            |
| Four constellation   |                 |               |               |
| 32 SVs   | 631             | 10            | 55            |
| 48 SVs   | 1330            | 10            | 87            |

**Table 3** Simulation configuration

| Simulation tools                | MAAST        |
|---------------------------------|--------------|
| $\sigma_{\text{URE},i}$         | 0.5 m        |
| $\sigma_{\text{URA},i}$         | 1 m          |
| $b_{\text{nom},i}$              | 0.75 m       |
| $P_{\text{sat},i}$              | $10^{-5}$    |
| $P_{\text{const},i}$            | $10^{-4}$    |
| Latitude and longitude interval | $10^\circ$   |
| Almanac format                  | Yuma almanac |
| GPS                             | Nominal 24   |
| GLONASS                         | Nominal 24   |
| Galileo                         | Global 30    |
| BDS                             | Global 35    |
| Area/user points                | Global/648   |
| Time duration                   | 24 h         |
| Time step                       | 1 h          |

The simulation software was developed based on the open source MATLAB Availability Analysis Simulation Tools (MAAST) provided by Stanford University (Jan et al. 2001). A total of 638 user points with  $10 \times 10$  latitude and longitude degree grids exist on the world map. The error model is adopted from GEAS (2008).

**Two-constellation situations**

Two-constellation situations using nominal 24 GPS satellites constellation and global 30 Galileo satellites constellation are considered as representative examples to obtain the results.

A comparison of the VPLs and EMTs obtained via the baseline MHSS and the OrbSel methods is shown in Fig. 4. The data for baseline MHSS and OrbSel are plotted on the x-axis and y-axis, respectively. The red points correspond to EMTs, and the blue ones represent VPLs. In the figure,

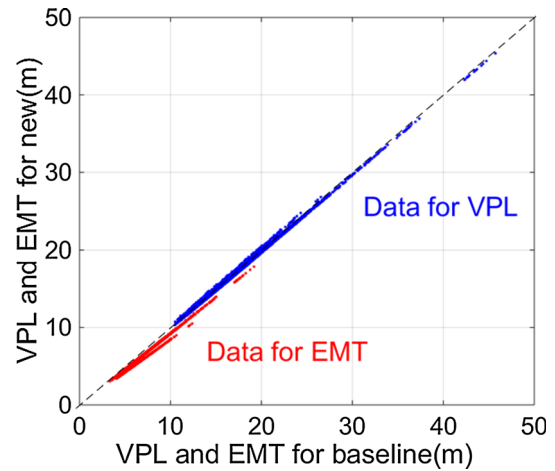


**Fig. 4** VPLs and EMTs for the baseline MHSS and the OrbSel method

both the VPLs and EMTs are close to a line with a slope of  $45^\circ$ . The OrbSel EMT is slightly less than the baseline MHSS EMT, since a smaller number of evaluating subsets decreases the threshold of the solution separation test. Moreover, the difference would be more obvious with increased subset disparity (Walter et al. 2014).

As shown in Fig. 5, VPLs are obtained using the baseline MHSS method and the ConOut method (Walter et al. 2014). The ConOut method evaluates only two one-constellation-out modes (vertical axis), whereas the baseline MHSS case evaluates all first-order modes (horizontal axis). Although the results are essentially identical, the reduced subset approach produces slightly lower VPLs. The effect of reducing the thresholds is dominant in this example.

Figure 6 shows the four quality factor distributions and the simulation points for the baseline MHSS and the OrbSel methods ( $648 \times 24$  data points in each figure). Blue points represent the baseline MHSS method, and red points correspond to the OrbSel method. A large number of data points results in an overlap region. It still can be seen that the difference between VPLs, HPLs, and  $\sigma_{\text{acc}}$ s derived by two methods is not great. Moreover, the  $\sigma_{\text{acc}}$  results are completely consistent. Generally, the OrbSel EMT is slightly smaller.

Figure 7 shows the global 99% availability coverage under the baseline MHSS and OrbSel methods. 99% availability means that ARAIM is available 99% of the time at the user grid point. The top and bottom panels present the results of the baseline MHSS method and the OrbSel method, respectively. For two constellations, the 99% availability coverage of both methods is not fully 100%, but the coverage results are essentially identical. Furthermore, the coverage of OrbSel method is slightly higher, which is related to the EMT results above.



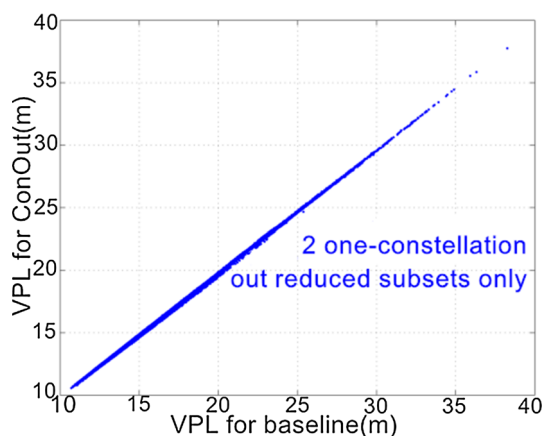


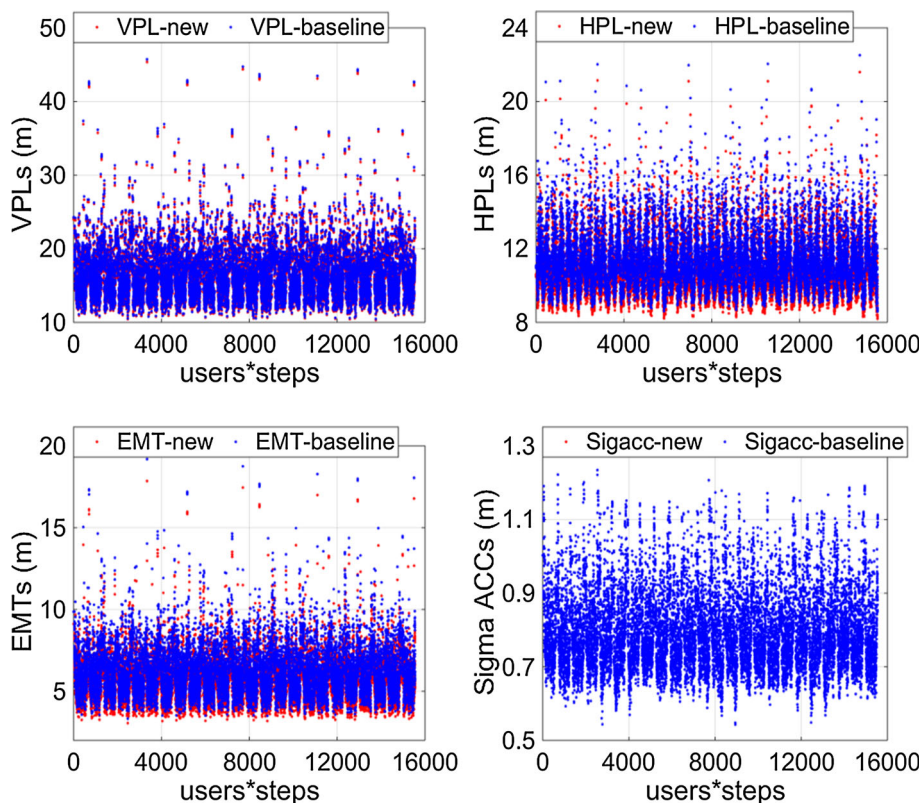
**Fig. 5** VPLs for the baseline MHSS and the ConOut method

According to the ARAIM availability, both the OrbSel and ConOut methods can replace the baseline MHSS method without producing a worse effect.

**Three-constellation situations**

To obtain the simulation results of three-constellation situations, the nominal 24 GPS satellite constellation, the global 30 Galileo satellite constellation and the global 35 BDS satellite constellation are utilized as a representative example.

**Fig. 6** Data distributions with simulation points for the two methods; *blue points* represent the baseline MHSS method, and *red points* correspond to the OrbSel method



The VPLs and EMTs obtained using the baseline MHSS and the OrbSel methods are shown in Fig. 8, where two sets of data points are basically gathered in the vicinity of the line with a slope of 45°. The distribution of the points above the line indicates that the results of the OrbSel method are greater than those of the baseline MHSS method, and vice versa. In addition, all EMTs remain less than 8 m, and all the VPLs remain less than 21 m.

Figure 9 shows the VPLs for the ConOut and baseline MHSS methods. The ConOut method is employed in two situations: (1) the red points correspond to using the one- and two-constellation-out subsets only; (2) the blue dots correspond to evaluating the three one-constellation-out and 2*N* one-constellation-out and one-satellite-out subsets, the VPL of which is nearly identical to that of the baseline MHSS case. Clearly, many false cases occur when a weak subset is used, and the VPL is significantly increased in situation 1. For the ConOut method, it is necessary to determine the number of subsets according to constellation performance. Furthermore, removing the entire constellation easily causes rapid deterioration of the geometry.

In the top-left, top-right and bottom-right panels of Fig. 10, the simulation point data for the baseline MHSS and the OrbSel methods are similar to that those in Fig. 6. Overall, the EMT results of OrbSel are smaller, and the difference is more significant than in the two- constellation situation.

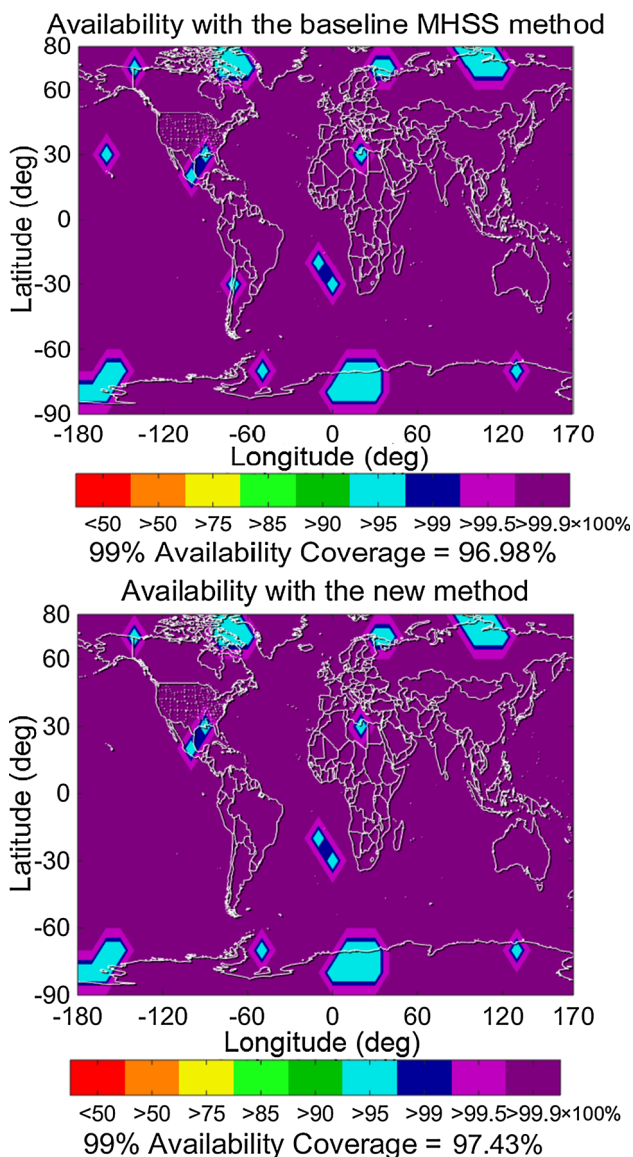


**Fig. 7** Global ARAIM availability as a function of user location under LPV-200 performance; for the baseline MHSS (*top panel*) and the ConOut method (*bottom panel*)

Although there are some differences in the results of the data, the baseline MHSS and the OrbSel method both provided 100% coverage of ARAIM availability. In three-constellation situations, ARAIM has better performance due to the increased number of satellites. The OrbSel method can replace the baseline MHSS method without any performance impact. The ConOut method performs well only when the  $(3 + 2N)$  subsets case is selected for evaluation.

**Four-constellation situations**

As for three-constellation situations, the nominal 24 GPS satellite constellation, the nominal 24 GLONASS satellite

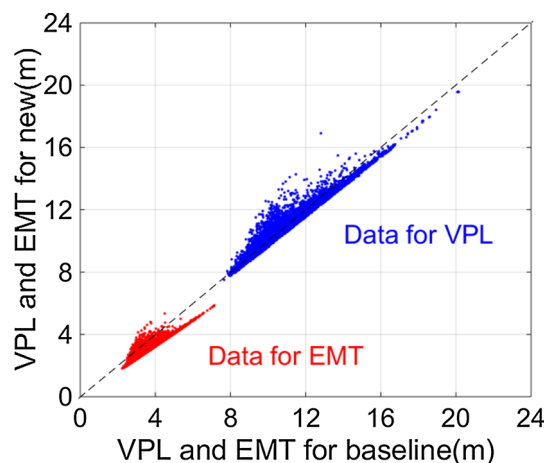


**Fig. 8** VPLs and EMTs for the baseline MHSS and the OrbSel method

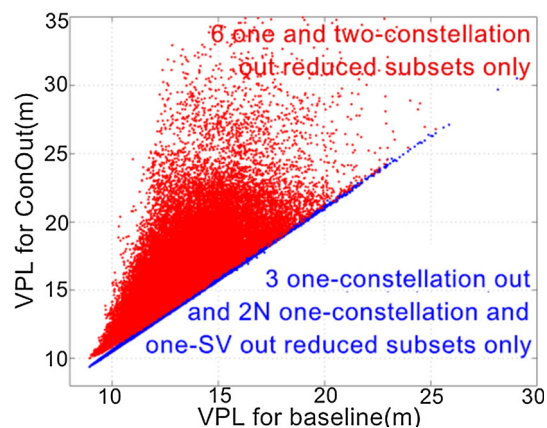


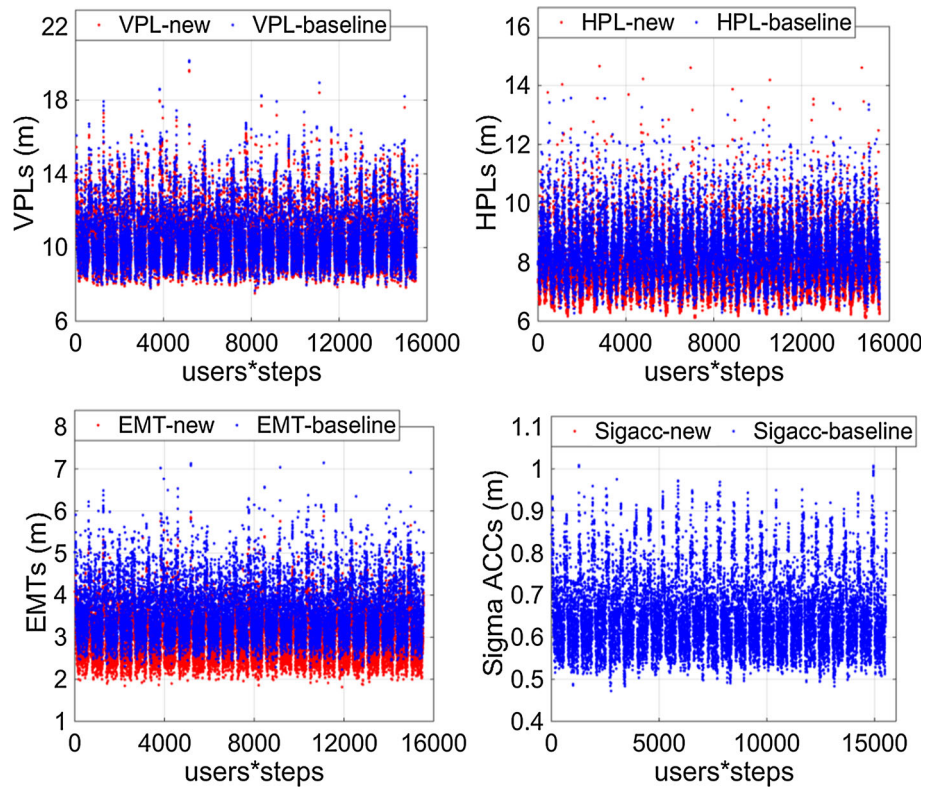
**Fig. 9** VPLs for the baseline MHSS and ConOut methods

constellation, the global 30 Galileo satellite constellation and the global 35 BDS satellite constellation are utilized as a representative example.

The VPLs and EMTs obtained using the baseline MHSS and the OrbSel methods are shown in Fig. 11. Obviously, the distribution of VPLs is similar to the situation of three constellations. Most of EMTs are below the line with a slope of  $45^\circ$ , and only a small part is above the line, indicating the much smaller EMT of the OrbSel method than the baseline MHSS method. Considering the data in Table 2, it can be inferred that the greater difference in the number of subsets between the two approaches leads to a more significant effect on the EMTs. However, the results of two methods are both better than the previous situations. Moreover, all the EMTs remain less than 5 m, and VPLs are less than 15 m.

In four-constellation situations, the comparison of the ConOut and baseline MHSS methods is shown in Fig. 12, with  $P_{const,j}$  set to  $10^{-3}$  and  $P_{sat,i}$  to  $10^{-4}$ . The ConOut method is evaluated with two selections of subsets: using

**Fig. 10** Data distributions with simulation points for the two methods; *blue points* represent the baseline MHSS method, and *red points* correspond to the OrbSel method



six two-constellation-out subsets only (red dots) and using ten one- and two-constellation-out subsets (blue dots). The VPLs of both selections are obviously greater than that of the baseline MHSS method. Although the availability can reach 100% coverage, part of the quality factor values reaches the margin, which makes the ARAIM system difficult to operate once a constellation is weak.

Figure 13 shows distributions of four quality factors and the simulation points for the baseline MHSS and OrbSel methods. In four-constellation situations, the VPLs, HPLs, and  $\sigma_{accs}$  of the two methods become increasingly similar,

even identical. As shown in the bottom-left panel of Fig. 13, the OrbSel EMT is still less than the baseline MHSS EMT. Moreover, the difference in the two data sets in the bottom-left panel of Fig. 13 is the most significant among the three simulation situations.

In four-constellation situations, the ARAIM availabilities of three approaches all achieve 100% coverage. The results of the OrbSel method are the closest to those of the baseline MHSS method. Generally, the results of the ConOut method are significantly greater than the baseline MHSS most of the time; this difference has a great influence on the geometry.

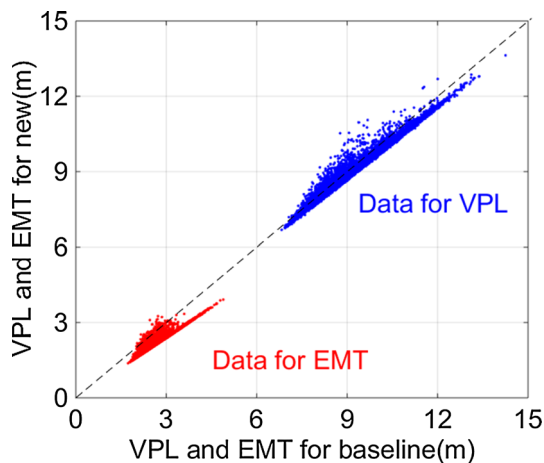


**Fig. 11** VPLs and EMTs for the baseline MHSS and OrbSel methods

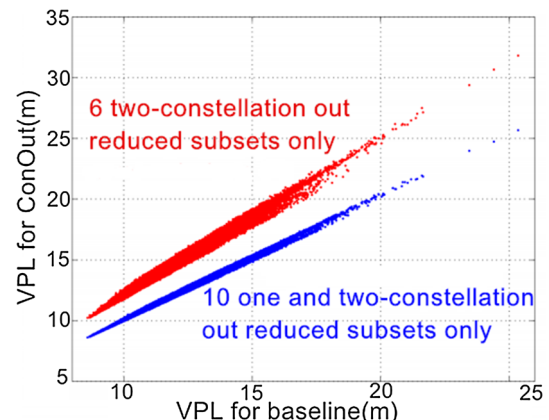
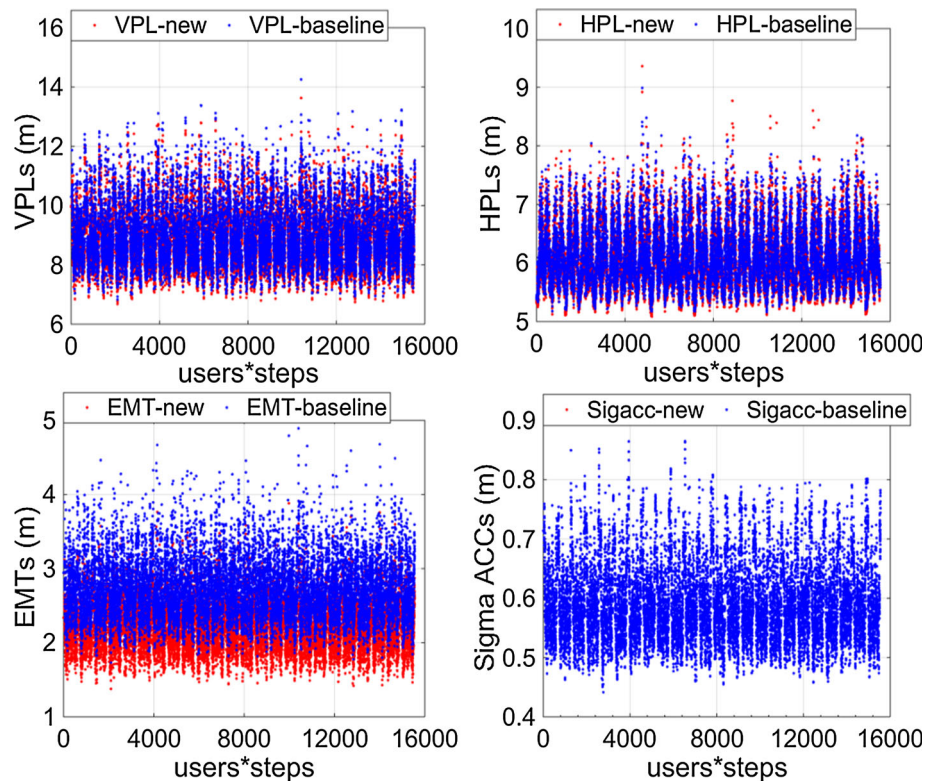


**Fig. 12** VPLs for the baseline MHSS and ConOut methods



**Fig. 13** Data distributions with simulation points for the two methods; *blue points* represent the baseline MHSS method, and *red points* correspond to the OrbSel method



## Conclusions

Based on the baseline MHSS and ConOut methods, we proposed a new optimal subset determination method based on orbit satellites. In the proposed method, the fault scope is narrowed by selecting the subsets of the constellation order that do not pass the threshold test or have the largest test statistic. Next, the subsets for the orbit order of the corresponding constellation were derived. Finally, the ARAIM monitoring subsets were calculated in three manners. The results indicated that the number of subsets for the OrbSel method is slightly greater than that of the ConOut method and significantly less than that of the baseline MHSS method. In the four constellations with 48 SVs, the number of subsets of the OrbSel method was found to be reduced by two orders of magnitude compared to that at baseline.

The simulation results of two-, three- and four-constellation situations illustrated the following: for two constellations, OrbSel and ConOut method have smaller VPLs and slightly higher global availability coverage than the baseline MHSS method; for three and four constellations, the results of OrbSel method are very similar to that of the baseline MHSS method. Although the global availability coverage of the two methods is 100%, the data results of the ConOut method are significantly greater than those of the baseline MHSS method, and some are at the edge of the Alarm Limit (AL), which is related to the rapidly

**Table 4** Average computational time for the baseline and OrbSel methods

| Simulation situation | Baseline MHSS method<br>Time/availability (%) | OrbSel method<br>Time/availability (%) |
|----------------------|---|--|
| Two constellation    | 2.5 s/96.98                                   | 3.5 s/97.43                            |
| Three constellation  | 17.5 s/100                                    | 6 s/100                                |
| Four constellation   | 28 s/100                                      | 8 s/100                                |

weakening geometry of the entire constellation. The ConOut method was found to have relatively high performance requirements regarding constellations. When a weak constellation exists, the obtained prediction results will be less ideal. In this case, the number of subsets must be increased according to the analysis.

Table 4 presents the average computational time of the baseline MHSS and the OrbSel methods for each simulation interval in the process of ARAIM availability prediction. The average computational time of the OrbSel method is significantly less than that of the baseline MHSS method, except for the two-constellation case, because of both the fewer number of subsets and the more steps in orbit order for the OrbSel method. For the OrbSel method, a higher number of constellations involved in the positioning means corresponds to more time savings, which is more conducive to real-time solutions.

Under the premise of availability, the OrbSel method reduced the number of subsets greatly, simplified the complexity of ARAIM algorithm, reduced the computational load, and guaranteed the geometry.

**Acknowledgements** The authors first thank Todd Walter, Juan Blanch, and Per Enge, whose study provided the authors with the ideas and foundations for the work we described, and their simulation results served as a reference for simulation analyses. The authors also thank the staff at the National Key Laboratory of CNS/ATM for their advice and interest. The work was conducted with financial support under the National Natural Science Foundation of China (Grant Nos. 61521091, 61501010, U1433114) and Aeronautics Science Foundation (Grant No. 2015ZC51035).

## References

- Blanch J, Walter T, Enge P, Lee Y, Pervan B, Ripp M, Spletter A (2012) Advanced RAIM user algorithm description: integrity support message processing, fault detection, exclusion, and protection level calculation. In: Proceedings of ION GNSS 2012, Institute of Navigation, Nashville, Tennessee, USA, Sept 2012, pp 2828–2849
- Cui XQ, Yang YX, Wu XB (2012) Influence of the orbital plane rotation angle on GEO satellite. *J Astronaut* 33(5):590–596
- Fan L, Jiang C, Hu M (2016) Ground track maintenance for BeiDou IGSO satellites subject to tesseral resonances and the luni-solar perturbations. *Adv Space Res* 59(3):753–761
- GEAS (2008) GNSS evolutionary architecture study, GEAS phase I-panel report. FAA, Washington
- GEAS (2010) GNSS evolutionary architecture study, GEAS phase II-panel report. FAA, Washington
- Jan SS, Chan W, Walter T, Enge P (2001) Matlab simulation toolset for SBAS availability analysis. In: Proceedings of ION GPS 2001, Institute of Navigation, Salt Lake City, UT, Sept 2001, pp 2366–2375
- Kaula WM (1966) Theory of satellite geodesy. Blaisdell Publishing Co., London
- Kropp V, Eissfeller B, Berz G (2014) Optimized MHSS ARAIM user algorithms: assumptions, protection level calculation and availability analysis. In: Proceedings of IEEE/ION PLANS 2014, IEEE, Monterey, California, July 2014, pp 308–323
- Langel S, Chan FC, Meno J, Joerger M, Pervan B (2013) Detecting earth orientation parameter (EOP) faults for high integrity GNSS aviation applications. In: Proceedings of ION ITM 2013, Institute of Navigation, San Diego, California, Jan 2013, pp 224–233
- Lee YC, McLaughlin MP (2007) Feasibility analysis of RAIM to provide LPV-200 approaches with future GPS. In: Proceedings of ION ITM 2007, Institute of Navigation, Fort Worth, TX, Sept 2007, pp 2898–2910
- Liu JY (2008) Principle and method of GPS satellite navigation and positioning. Science Press, Beijing
- Qian S, Li HN, Wu SG (2014) Perturbation compensation strategy for MEO non-resonant navigation constellation maintenance. *J Natl Univ Def Technol* 36(2):53–60
- Rippl M (2013) GNSS inter-constellation phasing: validation of the worst case assumption. In: Proceedings of ION ITM 2014, Institute of Navigation, San Diego, California, Jan 2013, pp 250–261
- Shah NH, Proulx RJ, Kantsiper B, Cefola PJ, Draim J (1998) Automated station-keeping for satellite constellations. *Adv Astronaut Sci* 97(1):275–297
- Starr MSB, Powe MD, Owen JIR (2004) A long-term statistical analysis of the accuracy of GPS and GLONASS broadcast orbit and clock models. In: Proceedings of ION GNSS 2004, Institute of Navigation, Long Beach, CA, Sept 2004, pp 2095–2103
- Van Dyke K, Kovach K, Lavrakas J, Carroll B, Systems O (2004) Status update on GPS integrity failure modes and effects analysis. In: Proceedings of ION NTM 2004, Institute of Navigation, San Diego, California, Jan 2004, pp 92–102
- Walker JG (1984) Satellite constellations. *Journal of the British Interplanetary Society* 37:559–572
- Walter T, Blanch J, Enge P (2014) Reduced subset analysis for multi-constellation ARAIM. In: Proceedings of ION ITM 2014, Institute of Navigation, San Diego, California, Jan 2014, pp 89–98
- Wang J, Ober P (2009) On the availability of fault detection and exclusion in GNSS receiver autonomous integrity monitoring. *J Navig* 62(2):251–261
- Wang ZP, Macabiau C, Zhang J, Escher AC (2014) Prediction and analysis of GBAS integrity monitoring availability at LinZhi airport. *GPS Solut* 18(1):27–40
- Working Group C (2012) Interim report of the EU/US cooperation on satellite navigation released. FAA. <http://www.gps.gov/policy/cooperation/europe/2013/working-group-c/>
- Working Group C (2015) Milestone 2 report of the EU/US cooperation on satellite navigation released. FAA. <http://www.gps.gov/policy/cooperation/europe/2015/working-group-c/>
- Working Group C (2016) Milestone 3 report of the EU/US cooperation on satellite navigation released. FAA. <http://www.gps.gov/policy/cooperation/europe/2016/working-group-c/>
- Zhi W, Wang ZP, Zhu YB, Li R (2016) Availability prediction method for EGNOS. *GPS Solut* 2016:1–13. doi:10.1007/s10291-016-0582-5



**Yishan Ge** received her B.S. in communication engineering from Shanghai University in 2015. She currently is a graduate student in the National Key Laboratory of CNS/ATM at Beihang University. Her research focuses on Advanced Receiver Autonomous Integrity Monitoring (ARAIM).





**Zhipeng Wang** received his B.S. in communication engineering from the School of Electronic Information and Engineering, Northwestern Polytechnical University (NWPU) in 2006 and received Ph.D. in Traffic Information Engineering from School of Electronic Information Engineering, Beihang University in 2013. He currently is a lecturer in the School of Electronic Information and Engineering, Beihang University. His

research focuses on the combination algorithms of Ground Based Augmentation System (GBAS) and Satellite-Based Augmentation System (SBAS) and on Advanced Receiver Autonomous Integrity Monitoring (ARAIM).



**Yanbo Zhu** received his B.S. and M.S. degrees from School of Electronic Information Engineering, Beihang University in 1992 and 1993, respectively. He is currently a Ph.D. candidate in School of Electronic Information Engineering, Beihang University and chief engineer of CNS/ATM labs, CAAC. His primary research interests are air traffic management, aeronautical telecommunication network, satellite navigation and automatic dependent

surveillance.